# Punching capacity of spread footings using aci 318-19 and the strip model

Lantsoght, Eva O.L.; Ospina, Carlos E.; Alexander, Scott D.B.

**DOI**
10.14359/51738756

**Publication date**
2023

**Document Version**
Final published version

**Published in**
Punching Shear of Concrete Slabs

**Citation (APA)**
Lantsoght, E. O. L., Ospina, C. E., & Alexander, S. D. B. (2023). Punching capacity of spread footings using aci 318-19 and the strip model. In A. Genikomsou, T. Hrynyk, & E. Lantsoght (Eds.), *Punching Shear of Concrete Slabs: Insights from New Materials, Tests, and Analysis Methods* (pp. 19-40). (American Concrete Institute, ACI Special Publication; Vol. SP-357). American Concrete Institute.
https://doi.org/10.14359/51738756

# PUNCHING CAPACITY OF SPREAD FOOTINGS USING ACI 318-19 AND THE STRIP MODEL

Eva O.L. Lantsoght, Carlos E. Ospina, and Scott D.B. Alexander

**Synopsis**: In design, the sectional depth of reinforced concrete spread footings is usually governed by design code provisions for punching shear, which are derived primarily from experiments on slab-column connections. Previous experiments have shown that the punching behavior of concentrically loaded spread footings differs from that of slab-column connections. This paper describes punching of a concentrically loaded spread footing by combining conventional strut and tie modeling with the concept of an arch strip, part of the Strip Model. By itself, the Strip Model describes the behavior of slab-column connections under a variety of loading conditions. For spread footings, Strip Model concepts need to be combined with conventional strut and tie modeling to adequately describe load transfer in a concentrically loaded spread footing. Two methods are explored, each producing closed-form expressions for the footing capacity that agree well with experimental results (112 tests from the literature). The analyses make it possible to estimate the fraction of footing load that is carried by conventional strut and tie behavior. The experimental results are also compared to punching shear capacities in accordance with ACI 318-19. The Strip Model produces results with roughly the same average test-to-predicted ratio (in the order of 1.3) as ACI 318-19 but with a lower coefficient of variation (10.3% compared to 15.8%). This work shows how a lower-bound plasticity-based model can be used for the practical case of determining the capacity of reinforced concrete spread footings failing in punching shear.

**Keywords:** arched strut, spread footings, punching shear, reinforced concrete, Strip Model

**Scott D. B. Alexander,** FACI, is a Professor of Practice in the Department of Civil and Environmental Engineering at the University of Alberta. He is an associate member of Joint ACI-ASCE Committees 421, Design of Reinforced Concrete Slabs, and ACI-ASCE Committee 445, Shear and Torsion, and its Subcommittee 445-C, Punching Shear. His research interests include structural applications of high-performance concrete, bridge rehabilitation, and punching shear.

ACI member **Eva O. L. Lantsoght** is a Full Professor at Universidad San Francisco de Quito, and an Assistant Professor at Delft University of Technology. She is the Vice Chair of ACI 445-0E Torsion, Secretary of ACI-ASCE 421, Design of Reinforced Concrete Slabs, member of ACI 445-0D Shear Databases, ACI 342, Evaluation of Concrete Bridges and Bridge Elements, and ACI-ASCE 445, Shear and Torsion, and an associate member of ACI 437, Strength Evaluation of Existing Concrete Structures.

**Carlos E. Ospina,** FACI, is Principal and Vice President, with Simpson Gumpertz & Heger Inc., Houston, TX, USA. He is a voting member of ACI 318 and Chair of ACI 318F (Foundations). As past Chair of ACI/ASCE 445C (Punching Shear) and member of *fib* WP 2.2.3 (Shear in Slabs) as well as co-editor of *fib* punching shear databases, he has contributed to the development of punching shear test databanks and design provisions in different codes.

## INTRODUCTION

In the design of spread footings, the dimensions in plan are usually dictated by the soil capacity. In North America, the sectional depth is chosen to satisfy punching shear provisions without relying on shear reinforcement. This process usually results in stocky members with low ratios of cantilever span to depth. While the flexural demand on spread footings can often be met with low flexural reinforcing ratios, the soil reaction pressure is generally one or two orders of magnitude larger than the typical design loads for suspended floors.

In most building codes, punching shear design provisions are the same for slab-column connections and spread footings. These design provisions have been derived for the most part from experiments on concentrically loaded, isolated slab-column specimens, often heavily reinforced. Whether such tests are sufficiently representative of spread footings is an open question. There is certainly evidence to suggest that there are differences between column-supported two-way slabs and footings. Experiments have shown that the shear span-to-depth ratio and thickness have a more significant influence on spread footings than on flat plates (Siburg and Hegger, 2014), and that the punching shear crack in spread footings tends to be steeper than in flat plates (Kueres et al., 2018).

ACI 318-19 acknowledges that, with regard to shear strength, footings constitute a special case. As a rule, expressions for one and two-way shear account for size effect; however, on the basis of Clause 13.2.6.2, neither the one-way nor two-way shear strengths of shallow foundations need to consider size effect. Possible explanations for this exclusion are that a significant fraction of the load is transferred by strut and tie behavior and/or the large transverse soil pressure acts as a quasi-shear reinforcement.

This paper examines the load transfer within a concentrically loaded square spread footing supporting a square column, although the principles can be applied to any spread footing (or even mat foundations). Such specimens account for the bulk of available test results. The capacities of the footing will be estimated using internal load transfer mechanisms that are compliant with material strength limits and are statically consistent. One of these internal load transfer mechanisms is conventional strut and tie behavior. The other is the arch strip, part of the Strip Model. The arch strip, only possible in two-way systems, is an extension to the strut and tie tool kit.

The Strip Model, originally developed (Alexander and Simmonds, 1992) for concentrically loaded two-way slab-column connections, has been successfully applied to a variety of problems concerning load transfer at column-slab connections and concentrated loads on slabs, including:

- combined shear and moment transfer at an interior column (Alexander, 2017, Afhami et al., 1998),
- edge column-slab connections (Alexander, 2017, Afhami et al., 1998),
- punching of two-way slabs with non-yielding reinforcement (Ospina et al., 2003),
- slab bridges under concentrated wheel loads (Lantsoght et al., 2017),
- miscellaneous design applications (Alexander and Lantsoght, 2018).

For a column-supported two-way slab, arch strips account for essentially all of the shear transferred from the slab to the column; the shear transferred by conventional strut and tie behavior is negligible. In contrast, the load supported by a footing is transferred through some combination of conventional strut and tie (direct) behavior and arch strip behavior. Because both of these load transfer mechanisms are based on lower-bound plasticity principles, the combination that produces the highest capacity is closest to being correct.

## RESEARCH SIGNIFICANCE

This work provides a rational representation of the mechanism of load transfer in spread footings by adding the arch strip concept to conventional strut and tie modeling. By themselves, both methods underestimate the punching capacity of a footing. The combination results in a better estimate of the punching capacity of a footing. Load transfer by conventional strut and tie is not sensitive to size effect. However, there are aspects within the load path of an arch strip that should be size-sensitive. Understanding the extent to which each of these load transfer mechanisms participates within a footing is an important step toward resolving the importance of size effect in footings. These insights allow the designer to identify critical details potentially reducing unsafe designs for cases where experimental results may not be available. For researchers, this work can refine research questions and help in the design of test specimens and instrumentation.

## ACI 318-19 PUNCHING SHEAR STRENGTH OF SPREAD FOOTINGS

According to ACI 318-19 (ACI Committee 318, 2019), the two-way shear strength of a spread footing is:

$$V_{c,ACI} = 4\sqrt{f_c'}b_o d \tag{1}$$

where $f_c'$ is the specified concrete compressive strength in psi, $b_o$ is the critical punching shear perimeter, $d$ is the average of the effective depth to the flexural reinforcement.

The critical perimeter is located at $d/2$ from the face of column and has the same shape as the column (i.e. rectangular critical perimeter around a rectangular column; circular critical perimeter around circular column). For a square column loading a spread footing concentrically, the critical punching shear perimeter becomes:

$$b_o = 4(c+d) \tag{2}$$

with $c$ the side dimension of the square column.

It is assumed that the soil reaction pressure acting within the critical perimeter does not contribute to shear stress on the critical perimeter. As a result, the shear demand on the critical perimeter for a square footing with side length $l_f$ supporting a square column of side length $c$ becomes:

$$V_{demand} = \frac{P_{col} \times (l_f{}^2 - (c+d)^2)}{l_f{}^2} \leq V_{c,ACI} \tag{3}$$

where $P_{col}$ is the total column load.

For comparison, the punching resistance of a column-supported two-way slab is not exempt from size effect. The shear capacity of a concentrically loaded slab-column connection is:

$$V_{c,ACI} = 4\lambda_s\sqrt{f_c'}\, b_o d \tag{4}$$

where $\lambda_s$ is given by

$$\lambda_s = \sqrt{\frac{2}{1+\frac{d}{10}}} \leq 1.0 \tag{5}$$

with $d$ in inches.

## BRIEF OVERVIEW OF STRIP MODEL

The Strip Model (Alexander, 2017) is a lower-bound, plasticity-based method to define potential load paths between a two-way slab and its supporting columns. The model uses an arch strip (called a radial strip prior to 2018) to handle the transition from the deep behavior in the slab near the column support to the slender behavior in the slab at locations farther from the column support. The arch strip is an addition to the strut and tie tool kit, and it can be used in

conjunction with conventional straight-line concrete compression struts. Unlike straight-line struts, arch strips are restricted to two-way flexural systems. The Strip model is also compatible with the Strip Method for the design of slabs of Hillerborg, but includes shear distress (Hillerborg, 1996, Hillerborg, 1975).

Figure 1(a) illustrates the application of the Strip Model to an isolated, column-slab connection, typical of many tests. The slab is subdivided into regions (arch strips and quadrants of two-way slab) that are broadly consistent with observed behavior of slab-column connections (deep behavior parallel to an arch strip and slender behavior perpendicular to the arch strip). Within each arch strip, load is carried to the column by the vertical component of an arched compression strut. Figure 1(b) shows a simplified set of internal forces and moments acting on the arch strip.

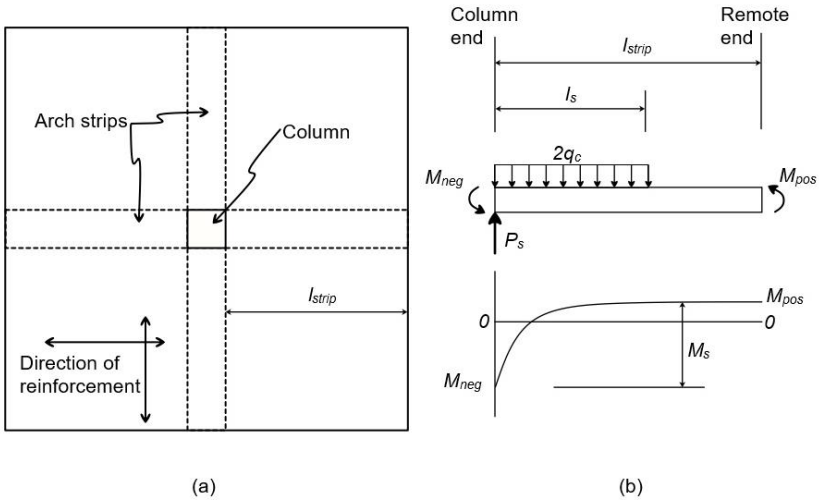


**Figure 1. Strip Model for concentric punching of a column-supported slab: (a) layout of arch strips, (b) equilibrium of internal loads**

Alexander and Simmonds (1992) show that with reasonable limits on the internal shears and moments shown in Fig. 1(b), simply satisfying equilibrium provides a safe and reliable estimate of the punching capacity of slab-column connection test specimens.

The reasonable limit on shear, labelled $q_c$, is the one-way slab shear. The factor 2 comes from the fact that the arch strip is loaded on two sides. The magnitude of $q_c$ is taken as:

$$q_c = 2\lambda_s\sqrt{f_c'}d \tag{6}$$

Consistent with ACI 318-19, $\lambda_s$ is given by Eq. (5). Note that for application to test results, the upper limit of 1.0 in Eq. (5) is removed to account for the beneficial effect of smaller sized test specimens.

A rectangular distribution of internal shear is the simplest distribution that does not violate the internal shear capacity of the slab. Afhami et al. (1998) use a non-linear finite element analysis to show that the stepped nature of the loading diagram is a reasonable approximation of the distribution of internal two-way plate shear, which is a combination of bending and torsional moment gradients.

The reasonable limits on negative and positive bending moments, $M_{neg}$ and $M_{pos}$, respectively, are those that are consistent with boundary conditions and can be resisted by a strip of slab of width $c$ (column dimension). For the majority of test specimens, the edges are unrestrained, forcing $M_{pos}$ to be zero; however, where the boundary conditions support a non-zero magnitude of $M_{pos}$, the strip model provides capacities that agree with test results.

$M_s$ is the total rotational support of the strip. It is the sum of $M_{neg}$ and $M_{pos}$ plus a possible torsional contribution from the side faces of the strip. For typical column-supported slabs, where the slab is slender and negligible load is

transferred by conventional strut and tie behavior, the benefit of torsional moment is accounted for by assuming a rectangular distribution of internal shear. Ignoring the additional contribution of torsional moment to $M_s$ has little impact on the predicted capacity of the connection.

It should also be noted that the loading diagram does not include load applied directly to the strip. This load could be included by replacing $q_c$ with an effective loading term given by:

$$q_{eff} = q_c + p \times {}^{c}/_{2} \tag{7}$$

where $p$ is the total distributed load acting on the slab. For column-supported slabs, the difference between $q_c$ and $q_{eff}$ is negligible. Ignoring this direct (or external) load on the strip always errs (slightly) on the safe side.

From static equilibrium, the capacity of one arch strip is:

$$P_s = 2\sqrt{(M_{s,neg} + M_{s,pos})q_c} = 2\sqrt{M_s q_c} \tag{8}$$

As is the case with any strut and tie model, the Strip Model provides a load carrying capacity that complies with material stress limits and satisfies internal equilibrium throughout. It does not predict a particular failure mechanism. There are many potential failure points that would result in the collapse of the load transfer regime described in the Strip Model.

The capacity of the arch strip is a function of both its flexural support, $M_s$, and its loading, $q_c$. This highlights a difference between what is generally built and what is often tested. Most two-way slabs in service have very little flexural reinforcement in excess of that needed for their design ultimate load. In contrast, slab specimens produced for shear tests often have excess flexural reinforcement, ostensibly to preclude a premature flexural failure.

## LOAD TRANSFER IN FOOTINGS

Spread footings share many of the attributes of suspended slabs or flat plates but there are some important differences. The depth of the footing, its relatively short cantilever span, and the magnitude of distributed load (the soil reaction, $q_{soil}$, is usually one or two orders of magnitude greater than the typical uniform load applied on a suspended slab) suggest that a significant fraction of shear transfer between column and footing should be by conventional strut and tie behavior.

The working hypothesis here is that the load transfer in a footing is by some combination of conventional strut and tie behavior and arch strip behavior. It is perhaps trivial to note that the soil reaction directly below the column must be carried by a direct compression field, a compression strut that requires essentially no tension tie. Outside of this region, there is the possibility for load to be shared between the direct strutting and the arch strip mechanisms. Within the footing, beyond the face of column, it is assumed that the fractions of load carried by the direct strutting and arch strip mechanisms are uniform. It may be that the face of column is not the optimum (i.e. leads to maximum predicted capacity) choice for such a boundary but it is a convenient place to start when analyzing test results.

For a square column supported by a square footing, the trapezoidal region of footing tributary to a single column face is shown in Figure 2. The total load carried by a single face of the column is:

$$P_{trib} = q_{soil}(a_f + c) \times a_f = q_{soil} \times A_{trib} \tag{9}$$

where $c$ is the column side dimension, $q_{soil}$ the soil pressure, $a_f$ is the cantilever span of the footing, and $A_{trib}$ is the area of footing tributary to one column face.

This total load is broken down into two portions: (1) $P_{direct}$ is the fraction carried by direct strutting and (2) $P_{strip}$ is the fraction carried by the arch strip mechanism. For equilibrium:

$$P_{direct} + P_{strip} = P_{trib} \tag{10}$$

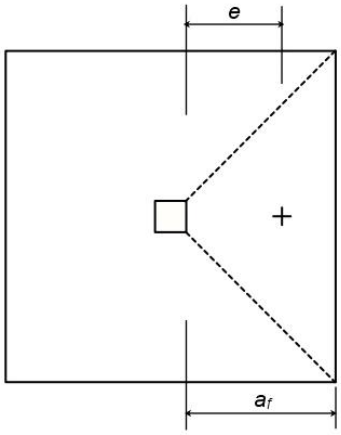


**Figure 2. Tributary area for loading to single face of column placed centrically on footing.**

**Load Carried by Direct Strutting, $P_{direct}$**

The fraction of load carried by direct strutting, $P_{direct}$, exerts a moment, $M_{direct}$, at the face of the column. $P_{direct}$ is the vertical component of the compression block associated with this moment.

$$M_{direct} = P_{direct} \times e \tag{11}$$

where $e$, the distance from the column face to the centroid of the tributary area, is given by:

$$e = a_f \left(\frac{1}{2} + \frac{a_f}{6(a_f+c)}\right) \tag{12}$$

**Load Carried by Arch Strip Behavior, $P_{strip}$**

Figure 3 shows the configuration of arch strips for a square footing supporting a square column under concentric load. Clearly there are similarities between Fig. 3 and Fig. 1 but there are some important differences. For a concentrically loaded, square column-slab connection, it is reasonable to assume that $P_s$ accounts for all of the load tributary to the column face and $M_s$ is 100% of the moments acting at the ends of a strip. In the case of a footing, $P_{strip}$ accounts for some as yet unknown fraction of $P_{trib}$. The rotational support for the strip, shown as $M_{strip}$, is an unknown fraction of the available moment capacity at the column end of the strip plus a possible contribution from torsional moments on the side faces.

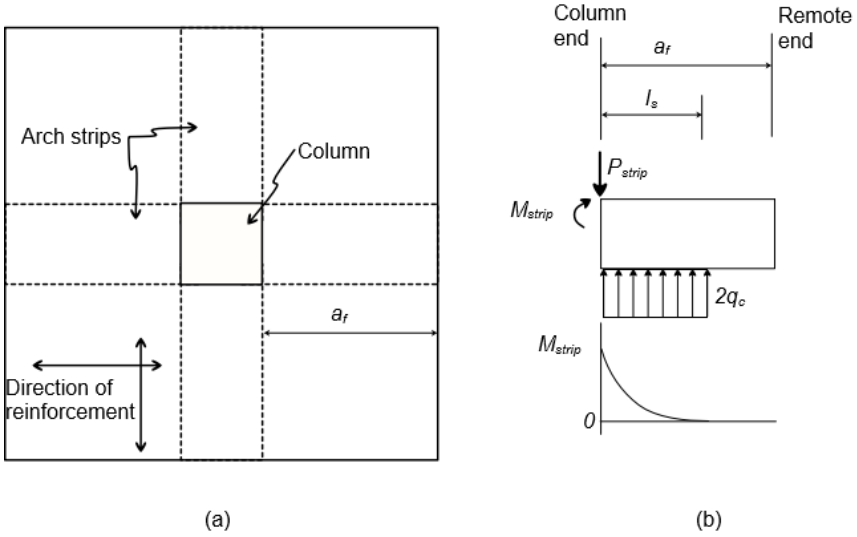


**Figure 3. Application of Strip Model to a spread footing: (a) layout of arch strips (b) internal loads**

As before, the relation between the rotational support of the strip and the load transferred at a column face is:

$$P_{strip} = 2\sqrt{M_{strip} \times q_c} \tag{13}$$

Eq. (13) can be re-arranged to give:

$$M_{strip} = \frac{P_{strip}^2}{4q_c} \tag{14}$$

As noted earlier for the case of a column-supported slab, there are two sources of rotational support for the strip. The first is a direct flexural bending moment $M_{f,strip}$, at the support end of the strip. The second is a torsional moment, $M_{t,strip}$ that develops on the side faces of the strip. The torsional moment, $M_{t,strip}$, will be discussed in more detail later.

**Combining Direct Strutting and Arch Strip Behavior**

The arch strip and direct strutting load paths generate different moment fields within the footing near the column. Each makes demands on the flexural moment capacity of the footing at the face of the column, $M_f$. A fundamental constraint is that the flexural demands on the direct strutting and arch strip mechanisms cannot exceed this flexural capacity.

$$M_{f,strip} + M_{direct} \leq M_f \tag{15}$$

Consistent with the principles of a lower bound model, the combination of arch strip and direct strutting behavior that predicts the largest capacity for the connection governs.

A three-step approach is taken here:

1. Estimate $M_f$ in a way that is consistent with conventional reinforced concrete design principles and accounts for a flexural compression block that is inclined at some angle relative to the reinforcement.
2. Account for the contribution of twisting (torsional) moments in the footing (two methods are presented) (ACI Committee 447, 2018)
3. Distribute $M_f$ between the direct strutting and arch strip load paths in such a way as to maximize the predicted capacity.

**Derivation of moment capacity**

The estimate of moment capacity, $M_f$, is based on a strain compatibility analysis at the column face, modified to account for the effect of a sloping compression strut. Figure 4 illustrates the conventional strain compatibility analysis on a beam. A linear distribution of strain is assumed with the maximum concrete compression strain, $\varepsilon_{c,max}$, set to the concrete crushing strain (0.003 in ACI 318-19). The concrete strength is $f_c'$ with stress block parameters $\alpha_1$ and $\beta_1$ as defined in ACI 318-19. The modulus of elasticity and yield strength of the steel reinforcement are $E_s$ and $f_y$, respectively, and the stress in the steel reinforcement is $f_s$.

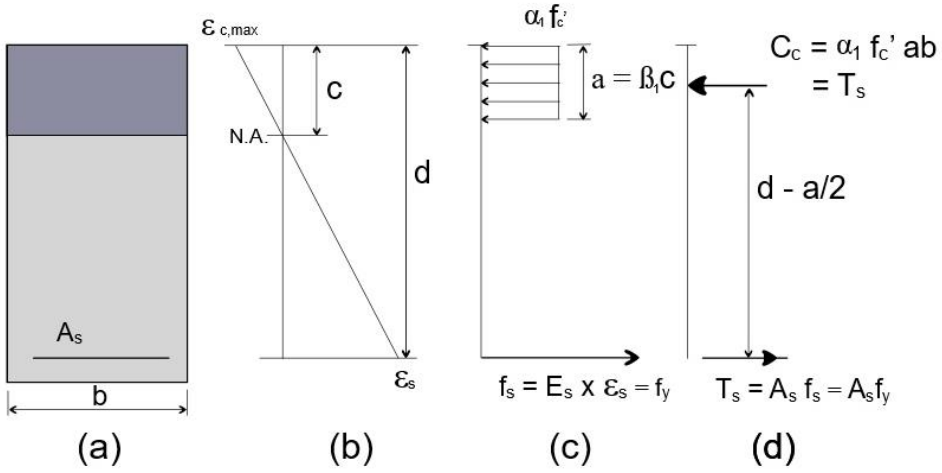


**Figure 4. Strain compatibility analysis: (a) cross-section; (b) strain diagram; (c) stresses; (d) force resultants.**

Where the steel strain is less than or equal to yield, enforcing longitudinal equilibrium produces a quadratic expression in $f_s$ (or $\varepsilon_s$). Incorporating the substitution $\varepsilon_{c,max} \times E_s = f_{cs}$, the solution of this quadratic equation is:

$$f_s = \frac{-f_{cs} + \sqrt{f_{cs}^2 + \frac{4\alpha_1\beta_1 f_c^{'} f_{cs} \times bd}{A_s}}}{2} \leq f_y \tag{16}$$

In the derivation of Eq. (16) it is assumed that the compression stresses are parallel to the tension reinforcement. This is rigorously true only if there is no shear. It remains a good approximation with non-zero shear as long as the section is well below balanced conditions. For heavily reinforced sections subject to combined shear and moment, Eq. (16) overestimates $f_s$ and hence, overestimates the moment capacity of the section.

Both direct strutting and the arch strip formulations involve inclined compression struts. Moreover, tests of footings tend to have generous flexural reinforcement. It is reasonable to consider the slope of the compression strut when estimating the moment capacity at the face of the column. Figure 5 shows the resultant compression strut (from direct strutting and arch strip behavior) at the face of the column load, inclined relative to horizontal at an angle $\theta$. Using conventional stress block parameters, the force resultant of the concrete under compression is:

$$C_c = \alpha_1 f_c^{'} ab \tag{17}$$

Because the strut is inclined, the vertical dimension of the stress block, $a_{eff}$, is equal to $a/\cos\theta$. The compression force in the resultant strut, $C_c$ can be expressed as:

$$C_c = \alpha_1 f_c^{'} a_{eff} \times \cos\theta \times b = \alpha_1 f_c^{'} \beta_1 c_{eff} \times \cos\theta \times b \tag{18}$$

Horizontal force equilibrium leads to:

$$H_c = T \tag{19}$$

$$C_c \cos\theta = T \tag{20}$$

Combining Eq. (18) and Eq. (20) gives:

$$\alpha_1 f_c^{'} \beta_1 c_{eff} \times \cos^2\theta \times b = T \tag{21}$$

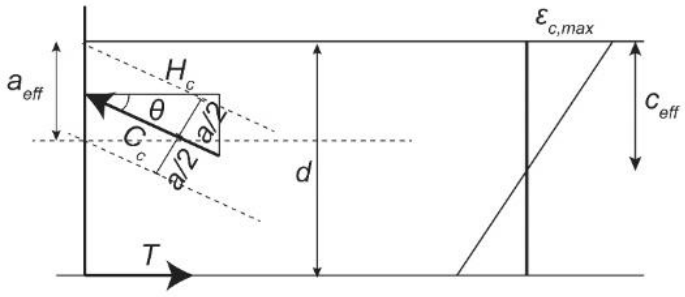


**Figure 5. Inclined strut and resulting effective height of the compression zone, $c_{eff}$**

The expression $cos^2\theta \times f_c'$ can be considered the apparent or effective concrete strength, $f'_{c,eff}$, when the flexural compression strut is inclined. Shear is carried by the vertical component of the strut. Implementing these concepts into Eq. (16) gives the expression:

$$f_s = \frac{-f_{cs} + \sqrt{f_{cs}^2 + \frac{4\alpha_1\beta_1 f_{c,eff}^{'} f_{cs} \times bd}{A_s}}}{2} \leq f_y \tag{22}$$

Here, $\theta$ is taken as 45°, which is consistent with observations from footing tests. As a result, $cos^2\theta = 0.5$ and $f'_{c,eff} = f_c'/2$. It follows that:

$$M_f = T \times \left(d - \frac{a_{eff}}{2}\right) \tag{23}$$

where $M_f$ is the flexural capacity at the face of the column, $T = A_s f_s$ and $a_{eff} = \frac{T}{\alpha_1 f'_{c,eff} \times b}$

To use Eqs. (22) and (23) to estimate the flexural capacity at the face of square column, the width of the compression block, $b$, is set to the column dimension, $c$.

**Incorporating twisting moments**

Slab twisting moments are unique to two-way systems. There are many statically admissible ways to account for twisting moments in a slab. Two will be considered here.

- **Method 1:** Increase the moment at the face of the column, $M_f$, by considering a band of reinforcement that is wider than the column dimension.
- **Method 2:** Incorporate a statically admissible distribution of twisting moment on the side faces of the arch strips.

In the text that follows, subscripts 1 and 2 are added to distinguish between the two approaches.

***Method 1***

Here it is assumed that the total rotational support for an arch strip is supplied by reinforcement within a band of width $c + d$. The reinforcement within this band defines the area of flexural reinforcement, $A_s$, to be used in Eq. (22). The flexural capacity, $M_{f,1}$, is given by Eq. (23).

With $M_{f,1}$ distributed between the direct strutting and arch strip mechanisms, Eq. (9) is rewritten as:

$$P_{trib,1} = P_{direct,1} + P_{strip,1} = \frac{\xi_1 M_{f,1}}{e} + 2\sqrt{(1-\xi_1) M_{f,1} q_c} \tag{24}$$

where $\xi_1$ is the fraction (for Method 1) of flexural moment at the column face to be engaged by direct strutting. It can be shown that the predicted capacity, $P_{trib,1}$, is maximum when:

$$\xi_1 = 1 - \frac{e^2 \times q_c}{M_{f,1}} \tag{25}$$

Making this substitution and simplifying produces:

$$P_{trib,1} = \frac{M_{f,1}}{e} + e \times q_c \tag{26}$$

***Method 2***

For this approach, only the reinforcement within the column width is assumed to contribute to $M_{f,2}$. Equations (22) and (23) are used to estimate this flexural capacity. As before, the flexural capacity at the column face, $M_{f,2}$, is split between the direct strutting and arch strip mechanisms.

Additional rotational support for the arch strip can come from twisting moment and its associated shear acting on the side faces of the strip.

$$P_{trib.2} = P_{direct,2} + P_{strip,2} = \frac{\xi_2 M_{f,2}}{e} + 2\sqrt{\left[(1-\xi_2) M_{f,2} + M_{t,strip}\right] q_c} \tag{27}$$

The total torsional moment, $M_{t,strip}$, acting on an arch strip will have two parts:

(1) $M_{twist,strip}$ is the integration of the distributed twisting moments acting on both faces of the arch strip.
(2) $M_{shear,strip}$ is the collateral moment generated by shear stresses that accompany the twisting moments in (1).

Regardless of how $M_{twist,strip}$ is distributed over the side face of the arch strip, its intensity must be zero at both ends. This is clearly the case anywhere on the free edge of the footing. At the column end of the arch strip, the intensity of twisting moment must be zero by symmetry; the side face of the arch strip is at the corner of the column, which lies on a diagonal axis of symmetry for the footing.

As long as $M_{twist,strip}$ varies in its intensity on the side faces of an arch strip, static equilibrium requires an associated set of shears, also acting on the side faces. Because the intensity of twisting moment is zero at both boundaries, the

associated shears must sum to zero; however, it can be shown from equilibrium that the shears generate a non-zero moment, $M_{shear,strip}$, that is precisely equal to $M_{twist,strip}$.

Figure 6 illustrates internal stress resultants for an arch strip with a limiting distribution of shear acting on its side faces. In a two-way flexural system, twisting moments are bending moments acting about an axis that is skewed to the coordinate axes. It follows that the magnitude of $M_{twist,strip}$ may be constrained by the bending capacity of the footing. Along the side face of an arch strip, twisting moment is also limited by the length over which the twisting moment is being generated and the shear capacity of the slab, $q_c$, which limits the maximum rate at which twisting moment can be generated.

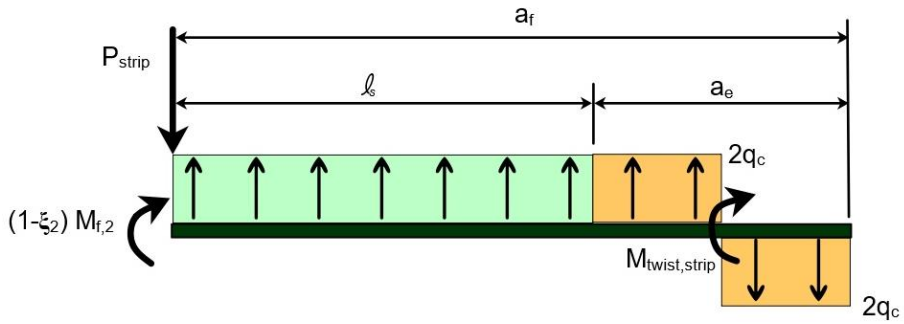


**Figure 6. Internal stress resultants with limiting distribution of shear.**

Implicit in Figure 6 is the assumption that twisting moment is limited by the shear capacity of the footing, $q_c$. For footings this is a good assumption because the length $a_e$ is short. However, other limits may govern. For example, where the length $a_e$ is long enough, the magnitude of the twisting moment may be limited by the bending capacity of the footing. Assuming a single mat of footing reinforcement, the upper limit for the quantity $\frac{a_e \times q_c}{2}$ is about ½ of the distributed bending strength of the footing.

From Fig. 6, the equal and opposite shears acting near the remote end of the strip generate the moment, $M_{shear,strip}$.

$$M_{shear,strip} = 2q_c \times \left(\frac{a_e}{2}\right)^2 = \frac{q_c a_e^2}{2} \tag{28}$$

Since $M_{shear,strip} = M_{twist,strip}$ it follows that:

$$M_{t,strip} = M_{shear,strip} + M_{twist,strip} = q_c a_e^2 \tag{29}$$

From equilibrium of the arch strip, the loaded length, $l_s$, is:

$$l_s = \sqrt{\frac{M_{f,strip} + M_{t,strip}}{q_c}} = \sqrt{\frac{(1-\xi_2)M_{f,2} + M_{t,strip}}{q_c}} \tag{30}$$

Unlike Method 1, a closed form solution to maximize the capacity predicted by Method 2 could not be found. Instead, an iterative approach was used, producing the somewhat surprising result that the total load is maximized if $\xi_2 = 1$. This leads to a number of simplifications.

$$a_e = l_s = \frac{a_f}{2} \tag{31}$$

$$P_{trib,2} = P_{direct,2} + P_{strip,2} = \frac{M_{f,2}}{e} + a_f q_c \tag{32}$$

**Footing capacity**

Equations (26) and (32) are very similar in structure. Both have a first term that is related to the direct strutting component of load and a second term that is related to the arch strip contribution. A surprising feature in these equations is that the load associated with the arch strip mechanism, derived on the basis of Eq. (13), now appears to

be at most softly dependent on flexure. In the case of Eq. (26), the term $M_{f1}/e$ accounts for all of the load transferred by direct strutting plus a fraction of the load transferred by the arch strip mechanism, making the arch strip mechanism softly dependent on flexure. For Eq. (32), the term $M_{f2}/e$ accounts only for all load transferred by direct strutting while $a_f q_c$ accounts for all load transferred through the arch strip mechanism. Here the arch strip mechanism is independent of flexure but there is the underlying assumption that slab torsion is governed by a limiting shear rather than a limiting moment capacity.

Using either Method 1 or Method 2 to estimate the shear transfer capacity at a single column face, Eq. (9) is rearranged to provide an estimate of the maximum distributed pressure, $q_{soil}$, that the footing can carry.

$$q_{cap,i} = \frac{P_{trib,i}}{a_f(a_f+c)} \tag{33}$$

with $i$ = 1 or 2 for method 1 or 2.

The total column load that can be supported by a spread footing is:

$$P_{footing,i} = 4 \times P_{trib,i} \times \frac{l^2}{l^2-c^2} \tag{34}$$

## SPREAD FOOTING EXPERIMENTS FROM THE LITERATURE

Hawkins and Ospina report a databank of 150 tests studying punching shear in spread footings with square columns (Hawkins and Ospina, 2022). Setting aside the rectangular footing tests (for which a special formulation would be required), the data was reduced to a total of 112 experiments for comparison with the previously discussed methods and the formulation presented herein. These experiments are mainly taken from work reported by (Hegger et al., 2006, Hegger et al., 2009, Siburg and Hegger, 2014, Simões et al., 2016, Richart et al., 1949, Richart, 1948a, Richart, 1948b).

Table 1 gives an overview of the ranges of parameters in the database, with l the side of the square footing, c the side of the square column, $a_f$/d the cantilever footing span-to-depth ratio with $a_f$ taken to the face of the column, d the effective depth, $\rho_l$ the longitudinal reinforcement ratio, $\rho_t$ the transverse flexural reinforcement ratio, $f_{ym}$ the measured yield strength of the reinforcement steel, and $f_{cm}$ the measured concrete cylinder compressive strength. All variables are the same as in the databank (Hawkins and Ospina, 2022).

**Table 1. Ranges of parameters in database. Conversion: 1 in = 25.4 mm, 1 psi = 0.007 MPa, 1 ksi = 6.9 MPa**

| Parameter | Min | Max |
|---|---|---|
| $l$ (in) | 35.4 | 106.3 |
| $c$ (in) | 5.91 | 21.00 |
| $a_f/d$ (-) | 1.23 | 4.38 |
| $d$ (in) | 5.91 | 23.23 |
| $\rho_l$ (%) | 0.29 | 1.25 |
| $\rho_t$ (%) | 0.00 | 0.54 |
| $f_{ym}$ (ksi) | 52.70 | 90.94 |
| $f_{cm}$ (psi) | 1960 | 5530 |

## COMPARISON TO EXPERIMENTAL RESULTS

### Overall comparison

Figure 7 shows a comparison between the punching shear capacity calculated in accordance with ACI 318-19 and the observed punching shear capacity from the tests. For this comparison, the average values of the material properties are used. The values of $V_{c,ACI}$ are calculated as given in Eq. (1), where $f_c'$ is replaced by the average concrete cylinder compressive strength. Consistent with Eq. (3), the soil reaction inside the critical shear perimeter is assumed not to contribute to shear demand; hence, $V_{test}$ is given by:

$$V_{test} = P_{test} - \frac{P_{test}}{l^2}(d+c)^2 \tag{35}$$

with $P_{test}$ the maximum externally applied load on the footing's column stub. The average value of $V_{test}/V_{c,ACI}$ is 1.33, with a standard deviation of 0.21 and a coefficient of variation (COV) of 15.8%. Ratios of test load to predicted load

range from 0.90 to 1.83, with the majority of tests on the safe side (i.e. greater than 1.0), as can also be seen by comparing the data points in Figure 7 with the bisector line.

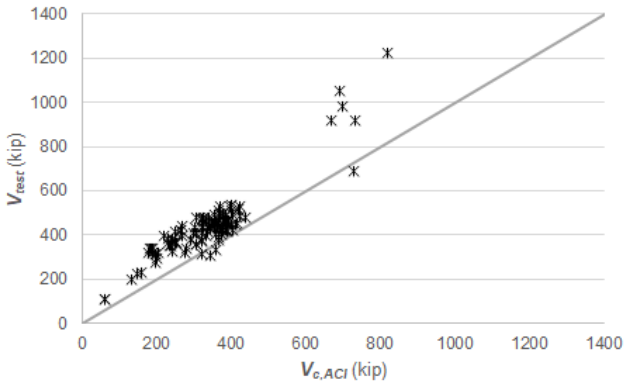


**Figure 7. Comparison between tested and predicted punching capacity using ACI 318-19. Conversion: 1 kip = 4.45 kN.**

Figure 8 compares test results with capacity predictions using Methods 1 and 2. Both lead to reasonable results. All predictions are on the safe side, as should still be expected for consistent and consequent combinations of two valid lower-bound load paths, namely the arch strip and conventional strut and tie. It appears there may be a trend with increasing soil pressure to more conservative predictions using Method 2 than with Method 1.

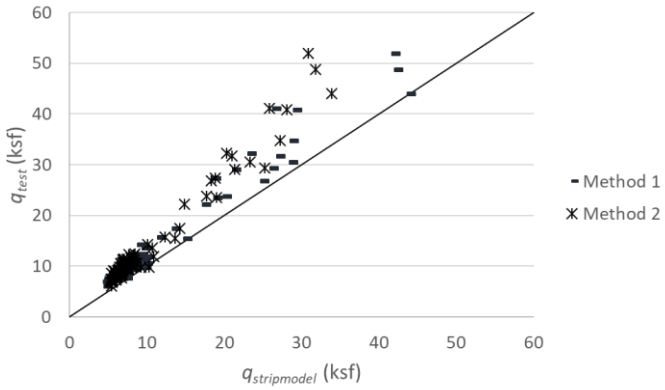


**Figure 8: Tested and predicted distributed load. Conversion: 1 ksf = 48 kPa.**

With Method 1, the average ratio of $q_{test}/q_{cap,1}$ is equal to 1.37 with a COV of 11.3%. Ratios of test load to predicted load range from 1.01 to 1.75. Using Method 2, the average ratio of $q_{test}/q_{cap,2}$ is equal to 1.39 with a COV of 9.9%. Ratios of test load to predicted load range from 0.96 to 1.68.

**Effect of Loading Intensity**

It was previously noted that an important difference between column supported two-way slabs and column-supporting spread footings is the intensity of distributed load carried by the two-way element. In the case of footings, the intensity of distributed load (i.e. soil pressure) is about two orders of magnitude greater than typical design loads for a column-supported slab.

In the overview of the Strip Model presented earlier, it was stated that the effect of distributed load on the arch strip itself can be included but that ignoring it would always err on the safe side (i.e. underestimate the capacity). In the case of column-supported slabs, where the intensity of distributed load is comparatively low, this error is small. The much higher distributed load in a footing suggests that the effect may not be negligible.

Incorporating the footing reaction requires reformulating the analysis with the slab shear capacity, $q_c$, replaced with the effective loading term, $q_{eff}$, as defined in Eq. (7). This requires iterative analyses for both approaches. These are named Method 1+ and Method 2+.

Reasonable approximations (within 2%) of the iterative results using Method 1+ and Method 2+ are obtained by a simple modification to Eqs. (26) and (32):

Method 1+: $$P_{trib,1+} \cong \frac{M_{f,1}}{e} + eq_c \times \frac{2.2}{2-\frac{e \times c}{A_{trib}}} \quad (36)$$

Method 2+: $$P_{trib,2+} \cong \frac{M_{f,2}}{e} + a_f q_c \times \frac{2}{2-\frac{a_f \times c}{A_{trib}}} \quad (37)$$

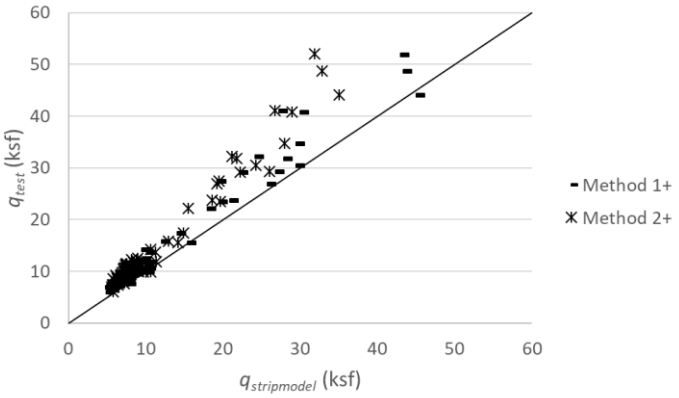


**Figure 9: Tested and predicted distributed load including contribution of distributed load on arch strip (iterative solution). Conversion: 1 ksf = 48 kPa.**

Figure 9 compares test results with capacities predicted by Methods 1+ and 2+, this time including the beneficial effect of distributed applied load on the arch strip. The plus sign indicates the iterative nature of the solution.

With Method 1+, the average ratio of $q_{test}/q_{cap,1}$ is equal to 1.28 with a COV of 10.5%. Ratios of test load to predicted load range from 0.98 to 1.60. Using Method 2+, the average ratio of $q_{test}/q_{cap,2}$ is equal to 1.31 with a COV of 9.7%. Ratios of test load to predicted load range from 0.92 to 1.63.

Comparing Fig. 8 and Fig. 9, the basic distribution of results appears to be about the same. The degree of conservatism introduced by ignoring the beneficial effect of distributed load on the arch strip is in the order of 6% to 7%. To avoid this additional bias, the balance of this work will be based on results using Methods 1+ and 2+.

**Fraction of load carried by direct strutting**

Whether one considers Method 1+ or Method 2+, the tributary reaction to one face of the column, $P_{trib}$, is carried through some combination of direct strutting and arch strip behavior. Figure 9 shows the estimated percentage of $P_{trib}$ that carried by direct strutting for each approach as a function of the cantilever span to depth ratio of the footing. The soil reaction directly below the column is not included here as it makes no demand on $M_f$.

While there is scatter in the results, Fig. 9 shows that to maximize the total capacity of the combined load transfer mechanisms (arch strip and conventional strut and tie), the fraction of load carried by conventional strut and tie must decrease as the span to depth ratio of the footing increases.

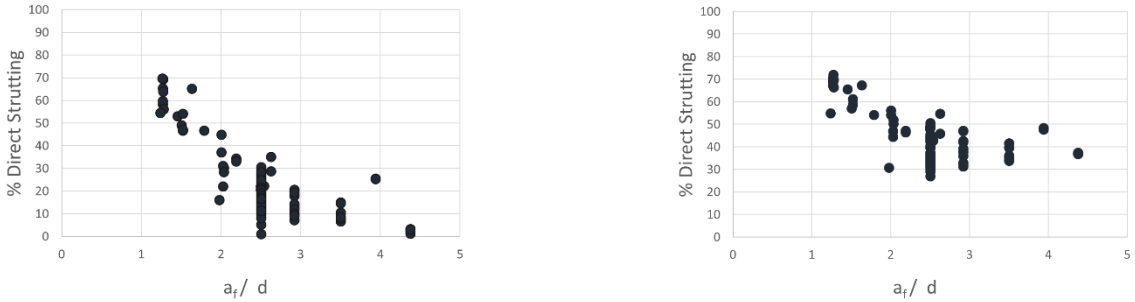


(a) Method 1+ (b) Method 2+

**Figure 10: Percent load attributed to conventional (direct) strut and tie behavior**

When the cantilever span-to-depth ratio, $a_f/d$, is about unity, both Method 1+ and 2+ appear to converge on a value of about 70% for the fraction of load transferred by direct strutting. For higher values of span to depth, Method 1+ consistently assigns a smaller fraction of the total load to direct strutting than does Method 2+.

The results for Method 1+ suggest that the contribution of direct strutting may be almost negligible for cantilever span to depth ratios exceeding approximately 5. Extrapolating the results for Method 2+ would suggest that the contribution of direct strutting becomes negligible at cantilever span to depth ratios exceeding something in the order of 8 to 10. For comparison, the cantilever span (face of column to midspan) to depth ratio of a column-supported two-way slab is typically greater than 10.

**Effect of Size**

Figure 11 shows the apparent influence of size for results using ACI 318-19 and Methods 1+ and 2+ from the Strip Model. The flexural depth of the footing is taken as the appropriate metric of size.

The Strip Model results shown here incorporate the size effect factor from ACI 318-19 (Eq.(6) for $\lambda_s$), albeit only for the fraction of total load assigned to the arch strip mechanism. The cap on $\lambda_s$ of 1.0 for flexural depths less than 10" is removed to capture the enhanced strength that is anticipated for thin footings. The load carried by direct strutting is unaffected by a size factor.

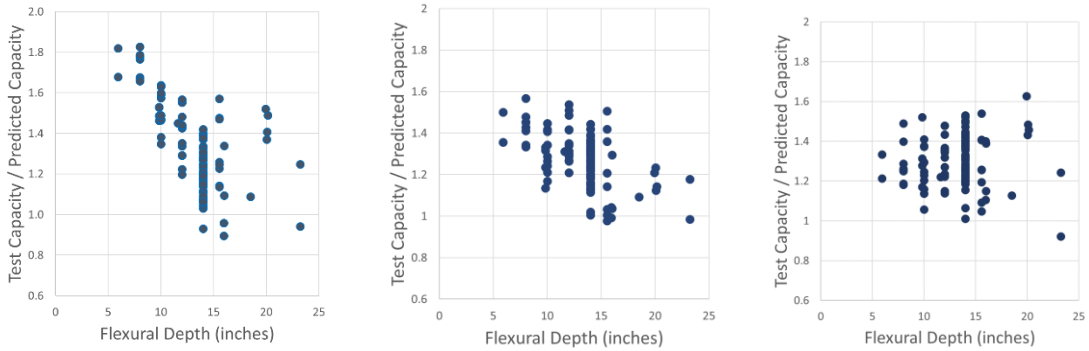


(a) ACI 318-19 (b) Strip Model - Method 1+ (c) Strip Model - Method 2+

**Figure 11: Influence of size. Conversion: 1 inch = 25.4 mm**

Both the ACI results and those for Method 1+ of the Strip Model appear to show some influence of size while those using Method 2+ seem largely insensitive. It is noted that, for the ACI results, the apparent sensitivity to size is in large part due to tests of specimens with flexural depths of 10 inches or less.

Both Strip Model approaches incorporate the same size effect factor in roughly the same way. This suggests that the difference in sensitivity to size may be the result of modeling rather than material property. Method 1+ bases its rotational support term, $M_s$, on a band of reinforcing ($c + d$) that is wider than the column face. It may be that using

this wider band of reinforcement introduces a model error that exaggerates the importance of flexural depth. Method 2+ has a torsional contribution that is more a function of the size of the footing.

On the other hand, the results for Method 1+ are less scattered for larger values of footing flexural depth, say greater than 14 inches. The trend to lower-than-expected capacities with larger flexural depths may even flatten for flexural depths greater than about 14 inches but these data are extremely limited. The maximum flexural depth in the data set is approximately 2 feet. Specimens with flexural depths less than about 14 inches are not representative of practice.

For the ACI results, the cantilever span to depth ratio may contribute to apparent size effect. Figure 12 shows calculated test to predicted capacities as a function of span to depth ratio. The results for the Strip Model show no real trend with this ratio.

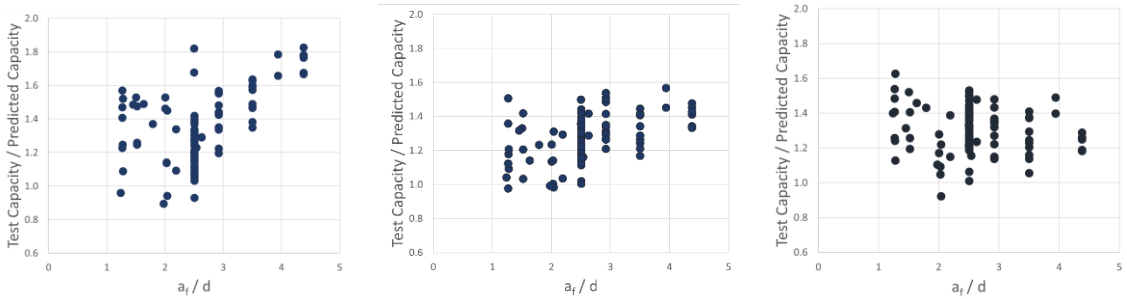


(a) ACI 318-19 (b) Strip Model - Method 1+ (c) Strip Model - Method 2+

**Figure 12: Influence of cantilever span to depth. Conversion: 1 inch = 25.4 mm**

The ACI results show some trend toward more conservative predictions of strength for larger values of cantilever span-to-depth ratio. In contrast, the results for the Strip Model show little variation with changing span to depth. Given the size constraints of laboratory testing, specimens with larger values of $a_f/d$ will tend to be those with smaller flexural depths. This suggests that some of the apparent size effect shown in the ACI results may be a result of modeling rather than material properties.

Table 2 presents a statistical comparison of the results. The results of using the simplified Methods 1 and 2 are included for comparison. The most striking observation of the results in Table 2 is that they are all very good, with coefficients of variation less than 16%. In Table 2 the characteristic value (5% lower bound of results assuming a normal distribution) is included for comparison.

**Table 2. Summary of Results (112 tests)**

| | ACI 318-19 | Strip Model | | | |
|---|---|---|---|---|---|
| | | Method 1 | Method 2 | Method 1+ | Method 2+ |
| AVG | 1.33 | 1.37 | 1.38 | 1.28 | 1.31 |
| STD | 0.21 | 0.15 | 0.14 | 0.13 | 0.13 |
| COV | 15.8% | 11.0% | 9.9% | 10.2% | 10.3% |
| Char | 0.98 | 1.12 | 1.16 | 1.06 | 1.09 |
| Min | 0.90 | 1.01 | 0.96 | 0.98 | 0.92 |
| Max | 1.83 | 1.72 | 1.68 | 1.57 | 1.63 |

## DISCUSSION

All of the variants of the Strip Model analyses presented here provide reasonable estimates of test results on footings. Maximizing the combination of two lower bound load transfer mechanisms, arch strips and conventional strut and tie, leads to estimated capacities that are generally safe. While the analyses give an indication of the distribution of load between the two lower bound mechanisms, they do not indicate which element within those mechanisms actually governed failure.

Rotational support is essential to both the arch strip and strut and tie mechanisms. Both mechanisms deliver a moment to the face of the column that is the couple formed by tension in the bottom mat reinforcement and the horizontal components of a strut, either arched or straight. The tension half of this couple can potentially be resisted by reinforcement across the width of the footing; however, the compression half of the couple is constrained to act within the width of the column face. The two mechanisms, arch strip and conventional strut and tie, must share the same concrete compression block.

The capacities of both the arch strip and conventional strut and tie load paths are based on satisfying global static equilibrium, subject to certain material constraints. The appropriateness of the material constraints, notably those that govern $q_c$ and $f_s$, may be questioned but, more importantly, it should be recognized that other factors, not expressly considered, could limit capacity. The most important such factor is bond or anchorage of flexural reinforcement.

A virtue of the arch strip mechanism is that it makes relatively modest demands for anchorage of the reinforcement that is tying the arch. In contrast, direct strut and tie behavior can make substantial demands on anchorage, especially for struts and ties that are picking up reaction near the edge of the footing. Figure 11 shows that, for the most part, the least conservative predictions by both Strip Model and ACI Code are for specimens with cantilever span-to-depth ratios less than 3. From Fig. 10, for span to depth ratios less than about 3, direct strutting starts to be the dominant load transfer mechanism. Anchorage failure may be a factor in some of the tests with less conservative predictions of capacity.

Conditions at the face of the column are estimated using a reduced concrete strength to account for the inclination of the compression strut (45°) combined with a strain compatibility analysis.

- An assumption of 45° is consistent with average observations of tests. It is tempting to say that the resultant angle is a function of the mix of arch strip and direct strut and tie behavior but this ignores the geometric constraint imposed by the column. Presumably, the design load for the column is present in the column where it meets its footing. The column is more or less uniformly, and heavily stressed over its full cross section. There may be a geometric constraint imposed by connecting the compression near the center of the column with a compression strut in the footing at the face of the column.
- The strain compatibility analysis is convenient but somewhat inconsistent with the assumed mechanics of load transfer for both arch strips and strut and tie. Both load paths, struts and ties and the arch strip, are meant to model load transfer in disturbed regions, where the distribution of strain through the depth of the section is not linear. The end result of the strain compatibility analysis is in reasonable agreement with test observations but it is not fundamentally consistent with behavior in a disturbed region.
- A consequence of the strain compatibility analysis used here is that many of the moment capacities at the face of the column end up being governed by compression failure of the concrete. As a result, while both the arch strip and conventional strut and tie mechanisms rely on reinforcing ties, the global static capacities are more affected by concrete strength than reinforcement yield.

The distribution of load between arch strip and conventional strut and tie maximizes the combined capacity of these two different load paths. For any particular test, using either Method 1+ or 2+, a consistent fraction of distributed load is assigned to direct strutting over the entire footing. This assumption simplifies calculations and seems to lead to reasonable results; however, it is likely that there are better internal distributions that have not been examined. For example, the combination of direct strutting within a certain distance from the column with arch strip behavior to pick up footing reaction farther away from the column is worth investigating. This is a topic for future research.

Apportioning capacity between the arch strip and strut and tie load paths may give useful insights into the role of size effect in footings. It is generally assumed that load transfer by conventional strut and tie is not subject to size effect, although this assumption does require some minimal level of ductility to preclude brittle fracture before the strut and tie mechanism can develop. It also seems intuitive that the proportion of load carried by direct strutting should increase as the cantilever span to depth ratio decreases, an intuition confirmed by Fig. 10.

It was noted that the results for ACI 318-19 shown in Fig. 11(a) appear to show some size effect. Much of this perception comes from tests of very shallow footings. The lowest values of test to predicted capacity are for specimens

with flexural depths of 14 inches or more. But it happens that these specimens correspond to those with cantilever span to depth ratios less than about 2.5, where direct strut and tie behavior should be significant.

There is a possibility that the ACI model for punching of footings itself introduces a measure of apparent size dependency. A similar observation was made comparing the results for Method 1+ and Method 2+. While it would be possible to "correct" the results shown in Fig. 11(a) with a size effect factor, that may be using a material property to compensate for a modeling error.

Of the two load transfer mechanisms used in the Strip Model analyses, only the arch strip is sensitive to size effect. The one-way slab shear strength, $q_c$, incorporates the ACI size factor $\lambda_s$ (for assessing test results, the upper limit of 1.0 is removed to account for enhanced strength expected from small-scale specimens). In the expression for strip capacity, shear term is under a root sign, substantially reducing the influence of size. If shear transfer is dominated by the arch strip mechanism, we would expect to observe a size effect in two-way systems that is the square root of what would be observed in one-way systems. In the case of footings, where the arch strip mechanism generally accounts for a fraction of the load, the apparent size effect should be even smaller.

Both Methods 1+ and 2+ provide reliable estimates of footing capacity. Equations (35) and (37) provide a convenient closed form (no iteration required) estimate of the capacity, which accounts for the beneficial effect of the soil reaction to the arch strip load transfer mechanism. Method 1+, with reinforcement within a width of $c + d$ defining the flexural capacity at the face of the column, is in line with the approaches used for detailing slab-column connections, and designers may be more comfortable with it. Method 2+, based on a direct estimate of torsional moments, may be more in line with the actual load path in the footing.

From the strain compatibility analysis, it can be seen that once a section is over-reinforced, the bending moment capacity $M_s$ is not very sensitive to the reinforcement ratio $\rho$. As a result, for the case of an over-reinforced section, both the flexural strength and the shear strength will be controlled by the concrete. This observation may explain why the ACI procedure leads to good predictions even though it does not explicitly address bending strength. However, there may be more to this.

It is worth noting that the ACI punching shear provisions were never intended to be an accurate model of behavior; instead, they were developed as a simple criterion to establish the boundary at which shear failure would govern over bending (Alexander and Hawkins, 2005). The presumption is that a designer will always provide sufficient flexural reinforcement for the design load. It is also presumed that the designer wishes to avoid shear failure. The only remaining design question is to locate the point at which capacity will no longer be governed by flexure. According to the Strip Model, the ACI concentric punching load identifies this cut-off point quite accurately for two-way column-supported slabs.

## SUMMARY AND CONCLUSIONS

The transfer of load between a spread footing and its supported column can be described by combining the load transfer concepts of the Strip Model with conventional strut and tie modeling. Two such models are presented. Each provides safe and reliable estimates of footing capacity when applied to 112 tests from the literature.

Due to their size and relative stockiness, spread footings tend to carry a larger proportion of the load through direct strutting action than slender two-way flexural systems, for which the Strip Model was originally envisioned. As a result, the contribution of this direct strutting action and slender arching action was studied in this paper.

The ACI 318-19 code expression for punching of footings provides very good estimates of footing strength, despite the fact that it was never intended to be a predictive model. These results appear to show some effect of size; however, this apparent size effect may be a consequence of anchorage failure of reinforcement and/or systematic bias in the analysis model rather than an additional material factor. The major drawback of the ACI procedure is that the fixed punching perimeter does not account for the contribution of the bending moment, which becomes increasingly important for cases with lower amounts of reinforcement that fail in flexure-induced punching (Mahamid et al., 2022, Ghali et al., 2015).

Both approaches of the Strip Model lead to accurate results, each with an average test to predicted capacity of about 1.3 and a coefficient of variation of 10.3%. The results are on the conservative side, which is in line with the expectation for a lower-bound plasticity-based model. For comparison with the ACI 318-19 punching expression results in roughly the same average test to predicted capacity but a slightly larger coefficient of variation (15.8%).

The results of this research show that the Strip Model concepts can also be applied to spread footings. The model is a powerful tool for researchers and designers. For designers, using the Strip Model as a tool helps them to better understand complex design situations, as well as optimize choices for reinforcement layouts. For researchers, the Strip Model can help with the preparation of experiments, to identify which types of specimens and which geometries and loading may be most interesting to test and understand. In addition, understanding the load paths can also guide researchers with the design of the instrumentation plan for the experiments.

## LIST OF NOTATIONS

| | |
|---|---|
| $a$ | height of concrete compressive stress block |
| $a_e$ | length of end segment of arch strip providing torsional support to strip |
| $a_{eff}$ | effect height of the compressive stress block |
| $a_f$ | cantilever span of the footing |
| $b$ | member width |
| $b_0$ | length of critical punching shear perimeter |
| $c$ | side dimension of the square column |
| $c_{comp}$ | height of the compression zone |
| $c_{eff}$ | effective height of the compression zone |
| $d$ | average of effective depth to the longitudinal and to the transverse flexural reinforcement |
| $e$ | distance between column face and centroid of footing area tributary to that face |
| $f_c'$ | specified concrete compressive strength |
| $f'_{c,eff}$ | effective concrete strength for calculation of moment, accounting for slope of compression strut |
| $f_{cm}$ | measured concrete cylinder compressive strength |
| $f_{cs}$ | equivalent concrete stress |
| $f_s$ | stress in the tension steel |
| $f_y$ | yield strength of steel |
| $f_{y,m}$ | measured yield strength of steel |
| $l$ | side dimension of the footing |
| $l_s$ | loaded length of strip |
| $l_{strip}$ | length of strip in Strip Model |
| $q_c$ | one-way shear capacity |
| $q_{cap,i}$ | estimate of distributed pressure the footing can carry using Method $i$ with $i$ = 1 or 2 |
| $q_{soil}$ | soil reaction |
| $q_{test}$ | distributed load reported in the test |
| $A_s$ | area of tension steel |
| $C_c$ | compressive resultant in cross-section |
| $E_s$ | Young's modulus of the reinforcement steel |
| $H_c$ | horizontal component of compression resultant |
| $M_s$ | total rotational support for arch strip in a column-supported slab |
| $M_f$ | flexural moment capacity of footing at face of the column |
| $M_{f,1}$ | flexural moment capacity of footing at face of the column using Method 1 |
| $M_{f,2}$ | flexural moment capacity of footing at face of the column using Method 2 |
| $M_{direct,}$ | cantilever moment generated by $P_{direct}$ |
| $M_{shear,strip}$ | collateral moment generated by shear stresses that accompany the twisting moments in $M_{s,twist}$ |
| $M_{strip}$ | total rotational support for an arch strip in a footing |
| $M_{t,strip}$ | total torsional moment acting on strip (has two equal parts: $M_{twist,strip}$ and $M_{shear,strip}$) |
| $M_{twist,strip}$ | integration of distributed twisting moments on both faces of the arch strip |
| $P_{cap}$ | total column load that can be supported by a spread footing using the Strip Model |
| $P_s$ | capacity of a single arch strip in a column-supported slab |
| $P_{direct}$ | load carried by direct strutting |
| $P_{direct,1}$ | load carried by direct strutting using Method 1 |

$P_{direct,2}$ load carried by direct strutting using Method 2
$P_{strip}$ load carried by single arch strip in footing
$P_{strip,1}$ $P_{strip}$ using Method 1
$P_{strip,2}$ $P_{strip}$ using Method 2
$P_{trib,i}$ estimate of footing capacity tributary to single face of the column, with subscript *i* indicating
$P_{trib,1}$ $P_{trib}$ using Method 1
$P_{trib,2}$ $P_{trib}$ using Method 2
$P_{test}$ total column load reported at failure of footing test specimen
$T$ tension resultant in cross-section
$V_{c,ACI}$ punching shear capacity of two way slabs according to ACI 318-19
$V_{test}$ calculated shear strength at *d* away from the column face
$\alpha_1$ factor to convert specified compressive strength to constant value of compressive stress in stress block
$\beta_1$ factor to convert height of compression zone to height of stress block, as function of concrete compressive strength
$\varepsilon_{c,max}$ crushing strain of concrete
$\varepsilon_s$ strain in the steel
$\varepsilon_y$ yield strain of steel
$\lambda_s$ size effect factor for shear from ACI 318-19
$\rho$ reinforcement ratio
$\rho_l$ longitudinal flexural reinforcement ratio
$\rho_t$ transverse flexural reinforcement ratio
$\theta$ angle of inclination of the compression strut
$\xi_1$, $\xi_2$ fraction of flexural moment at the column face engaged by direct strutting

## REFERENCES


ACI COMMITTEE 318 2019. *Building code requirements for structural concrete (ACI 318-19) and commentary,* Farmington Hills, MI, American Concrete Institute.

ACI COMMITTEE 447 2018. Design Guide for Twisting Moments in Slabs. Farmington Hills, MI: American Concrete Institute.

AFHAMI, S., ALEXANDER, S. D. B. & SIMMONDS, S. H. 1998. *Strip model for capacity of slab-column connections,* Edmonton, Dept. of Civil Engineering, University of Alberta.

ALEXANDER, S. D. B. 2017. Shear and Moment Transfer at Slab Column Connections. *ACI-fib international symposium: Punching shear of structural concrete slabs***,** 1-22.

ALEXANDER, S. D. B. & LANTSOGHT, E. O. L. 2018. The Arched Strut - a Tool for Modelling Column-Slab Connections. *IABSE 2018.* Nantes, France.

ALEXANDER, S. D. B. & SIMMONDS, S. H. 1992. Bond Model for Concentric Punching Shear. *ACI Structural Journal,* 89**,** 325-334.

GHALI, A., GAYED, R. B. & DILGER, W. 2015. Design of Concrete Slabs for Punching Shear: Controversial Concepts. *Structural Journal,* 112.

HAWKINS, N. M. & OSPINA, C. E. 2022. Effect of Flexural Reinforcement Ratio, Effective Depth and Slenderness Ratio on Punching Strength of Spread Footings. *ACI SP 353 - A. Ghali Symposium*.

HEGGER, J., RICKER, M. & SHERIF, A. G. 2009. Punching Strength of Reinforced Concrete Footings. *ACI Structural Journal,* 106.

HEGGER, J., SHERIF, A. G. & RICKER, M. 2006. Experimental Investigations on Punching Behavior of Reinforced Concrete Footings. *ACI Structural Journal,* 103.

HILLERBORG, A. 1975. *Strip Method of Design,* Wexham Springs, Slough, England, Viewpoint Publications, Cement and Concrete Association.

HILLERBORG, A. 1996. *Strip method design handbook,* London ; New York, E & FN Spon.

KUERES, D., RICKER, M. & HEGGER, J. 2018. Improved Shear Reinforcement for Footings—Maximum Punching Strength. *ACI Structural Journal,* 115.

LANTSOGHT, E. O. L., VAN DER VEEN, C., DE BOER, A. & ALEXANDER, S. D. B. 2017. Extended Strip Model for Slabs under Concentrated Loads. *ACI Structural Journal,* 114**,** 565-574.

MAHAMID, M., GAYED, R. B. & (EDITORS) 2022. SP-353: Design of Slabs for Serviceability and Punching Shear Strength: Honoring Professor Amin Ghali. *ACI Symposium Publication,* 323.

OSPINA, C. E., ALEXANDER, S. D. B. & CHENG, J. J. R. 2003. Punching of Two-Way Concrete Slabs with Fiber-Reinforced Polymer Reinforcing Bars or Grids. *ACI Structural Journal,* 100**,** 589-598.
RICHART, F. E. 1948a. Reinforced Concrete Wall and Column Footings: part 1. *ACI Journal Proceedings,* 45**,** 97-127.
RICHART, F. E. 1948b. Reinforced Concrete Wall and Column Footings: part 2. *ACI Journal Proceedings,* 45**,** 237-260.
RICHART, F. E., SHANNON, W. L. & BRYAN, R. H. 1949. Reinforced Concrete Wall and Column Footings: discussion and author's closure. *ACI Journal Proceedings,* 45**,** 260.1-260.3.
SIBURG, C. & HEGGER, J. 2014. Experimental investigations on the punching behaviour of reinforced concrete footings with structural dimensions. *Structural Concrete,* 15**,** 331-339.
SIMÕES, J. T., BUJNAK, J., RUIZ, M. F. & MUTTONI, A. 2016. Punching shear tests on compact footings with uniform soil pressure. *Structural Concrete,* 17**,** 603-617.

## ANNEX 1: EXAMPLE

**Description and general information**

The methodology is illustrated with experiment DF6 by Hegger et al. (2009). In this case, a square footing of $l$ = 47.25 in (1200 mm) with an effective depth $d$ of 15.55 in (395 mm) is loaded with a square column stub of 7.87 in (200 mm). The concrete compressive strength is given as 2760 psi (19.0 MPa) and the reinforcement ratio is 0.87% with a yield strength of 79 ksi (552 MPa) for the steel reinforcement. The footing failed at $P_{test}$ = 638 kips (2840 kN). This failure load corresponds to a value of the soil pressure $q_{soil}$ of

$$q_{soil} = \frac{P_{test}}{l^2} = \frac{638kips}{(47.25in)^2} = 41.12ksf$$

The authors also indicated $P_{flex}$ = 1607 kips (7147 kN). Since the failure load is far from the flexural capacity, the failure mode is identified as a brittle punching failure.

From the given geometry, the value of $a_f$ can be found as 19.69 in (500 mm), so that $a_f/d$ = 1.266. The value of $V_{test}$ at $d/2$ can be determined as:

$$V_{test} = P_{test} - \frac{P_{test}}{l^2}(d+c)^2 = 638kips - \frac{638kips}{(47.25in)^2}(15.55in + 7.87in)^2 = 480.9kips$$

**Capacity with ACI 318-19**

The punching shear capacity according to ACI 318-19 can be determined with the following value for the punching perimeter:

$$b_o = 4(c+d) = 4(7.87in + 15.55in) = 93.68in$$

The punching capacity then becomes:

$$V_{c,ACI} = 4\lambda_s\sqrt{f_c'}b_o d = 4\sqrt{2760psi} \times 93.68in \times 15.55in = 306.1kips$$

Given $V_{test}$ = 480.9 kips the value of $V_{test}/V_{ACI}$ becomes 1.57.

**Strip method solution**

***General concepts***

The shear capacity at the interface of the quadrant and strip is determined as:

$$q_c = 2\sqrt{f_c'}d\lambda_s = 2\sqrt{2760psi} \times 15.55in \times \sqrt{\frac{2}{1+\frac{15.55}{10}}} = 1.446\frac{kips}{in}$$

The eccentricity is determined as:

$$e = \frac{3a_f l - 2a_f^2}{6(l-a_f)} = \frac{3 \times 19.69in \times 47.25in - 2(19.69in)^2}{6(47.25in - 19.69in)} = 12.19in$$

***Capacity with Method 1+***

Assuming a band width of $c + d$ = 7.87 in + 15.55 in = 23.42 in, the reinforcement area in the band can be determined as:

$$A_s = \rho \times (c+d)d = 0.87\% \times 23.42in \times 15.55in = 3.168in^2$$

The stress in the steel can then be determined as:

$$f_s = \frac{-f_{cs} + \sqrt{f_{cs}^2 + \frac{4\alpha_1\beta_1 f'_{c,eff} f_{cs} \times bd}{A_s}}}{2}$$

$$= \frac{-87ksi + \sqrt{(87ksi)^2 + \frac{4 \times 0.85 \times 0.9 \times 0.5 \times 2760psi \times 87ksi \times 7.87in \times 15.55in}{3.168in^2}}}{2}$$

$$= 30.25ksi$$

The height of the compressive stress block is

$$a_{eff} = \frac{A_s f_s}{\alpha_1 f'_{c,eff} \times b} = \frac{3.168in^2 \times 30.25ksi}{0.85 \times 0.5 \times 2760psi \times 7.87in} = 10.38\ in$$

The resulting bending moment is:

$$M_{f,1} = A_s f_s \times \left(d - \frac{a_{eff}}{2}\right) = 3.168in^2 \times 30.25ksi \left(15.55in - \frac{10.38in}{2}\right) = 82.74kip - ft$$

The maximum load can then be determined as:

$$P_{trib,1+} = \frac{M_{f,1}}{e} + eq_c \times \left(\frac{2.2}{2 - \frac{e \times c}{A_{trib}}}\right)$$

$$= \frac{82.7kip - ft}{12.19in} + 12.19in \times 1.446\frac{kips}{in} \times \left(\frac{2.2}{2 - \frac{12.19in \times 7.87in}{19.69in \times (19.69in + 7.87in)}}\right) = 102.7kip$$

This value can be expressed as the following capacity:

$$q_{cap,1+} = \frac{P_{trib,1+}}{a_f(a_f + c)} = \frac{102.7kip}{19.69in(19.69in + 7.87in)} = 27.25ksf$$

The ratio of tested to predicted capacity is 41.12 ksf /27.25 ksf = 1.51

***Capacity with Approach 2+***

Assuming a band width of $c$ = 7.87 in, the reinforcement area in the band can be determined as:

$$A_s = \rho cd = 0.87\% \times 7.87in \times 15.55in = 1.065in^2$$

The stress in the steel can then be determined as:

$$f_s = \frac{-f_{cs} + \sqrt{f_{cs}^2 + \frac{4\alpha_1\beta_1 f'_{c,eff} f_{cs} \times bd}{A_s}}}{2}$$

$$= \frac{-87ksi + \sqrt{(87ksi)^2 + \frac{4 \times 0.85 \times 0.9 \times 0.5 \times 2760psi \times 87ksi \times 7.87in \times 15.55in}{1.065in^2}}}{2}$$

$$= 68.08ksi$$

The height of the compressive stress block is

$$a_{eff} = \frac{A_s f_s}{\alpha_1 f'_{c,eff} \times b} = \frac{1.065in^2 \times 68.08ksi}{0.85 \times 0.5 \times 2760psi \times 7.87in} = 7.85in$$

The resulting bending moment is:

$$M_{f,2} = A_s f_s \times \left(d - \frac{a_{eff}}{2}\right) = 1.065in^2 \times 68.08ksi \left(15.55in - \frac{7.85in}{2}\right) = 70.21kip - ft$$

The maximum load can then be determined as:

$$P_{trib,2+} = \frac{M_{f,2}}{e} + a_f q_c \times \left( \frac{2}{2 - \frac{a_f \times c}{A_{trib}}} \right)$$

$$= \frac{70.21kip - ft}{12.197in} + 19.69in \times 1.446 \frac{kips}{in} \times \left( \frac{2}{2 - \frac{19.69in \times 7.87in}{19.69in \times (19.69in + 7.87in)}} \right) = 102.3kip$$

This value can be expressed as the following capacity:

$$q_{cap,2+} = \frac{P_{trib,2+}}{a_f(a_f + c)} = \frac{102.3kip}{19.69in(19.69in + 7.87in)} = 27.15ksf$$

The ratio of tested to predicted capacity is 41.12 ksf /27.15 ksf = 1.52.